Phase behavior of the modified-Yukawa fluid and its sticky limit

Elisabeth Schöll-Paschinger, Néstor E. Valadez-Pérez, Ana L. Benavides, and Ramón Castañeda-Priego

Citation: J. Chem. Phys. **139**, 184902 (2013); doi: 10.1063/1.4827936
View online: http://dx.doi.org/10.1063/1.4827936
View Table of Contents: http://jcp.aip.org/resource/1/JCPSA6/v139/i18
Published by the AIP Publishing LLC.

Phase behavior of the modified-Yukawa fluid and its sticky limit

Elisabeth Schöll-Paschinger,[1,a)] Néstor E. Valadez-Pérez,[2,b)] Ana L. Benavides,[2,c)] and Ramón Castañeda-Priego[2,d)]

[1]*Department für Materialwissenschaften und Prozesstechnik, Universität für Bodenkultur, Muthgasse 107, A-1190 Wien, Austria*

[2]*División de Ciencias e Ingenierías, University of Guanajuato, Loma del Bosque 103, 37150 León, Mexico*

(Received 29 July 2013; accepted 18 October 2013; published online 8 November 2013)

Simple model systems with short-range attractive potentials have turned out to play a crucial role in determining theoretically the phase behavior of proteins or colloids. However, as pointed out by D. Gazzillo [J. Chem. Phys. **134**, 124504 (2011)], one of these widely used model potentials, namely, the attractive hard-core Yukawa potential, shows an unphysical behavior when one approaches its sticky limit, since the second virial coefficient is diverging. However, it is exactly this second virial coefficient that is typically used to depict the experimental phase diagram for a large variety of complex fluids and that, in addition, plays an important role in the Noro-Frenkel scaling law [J. Chem. Phys. **113**, 2941 (2000)], which is thus not applicable to the Yukawa fluid. To overcome this deficiency of the attractive Yukawa potential, D. Gazzillo has proposed the so-called modified hard-core attractive Yukawa fluid, which allows one to correctly obtain the second and third virial coefficients of adhesive hard-spheres starting from a system with an attractive logarithmic Yukawa-like interaction. In this work we present liquid-vapor coexistence curves for this system and investigate its behavior close to the sticky limit. Results have been obtained with the self-consistent Ornstein-Zernike approximation (SCOZA) for values of the reduced inverse screening length parameter up to 18. The accuracy of SCOZA has been assessed by comparison with Monte Carlo simulations. © *2013 AIP Publishing LLC*. [http://dx.doi.org/10.1063/1.4827936]

I. INTRODUCTION

During the last few years an increasing number of studies has focused on the understanding of the phase behavior of systems with very short-ranged attractive interactions.[1–8] Simple model systems with narrow attractive interactions, like square-well or hard-core attractive Yukawa systems, have turned out to play a crucial role when one tries to understand the phase behavior of protein and colloidal solutions, where the range of the effective interaction is significantly smaller than the particle diameter that is of nano- or microscopic size.[9–11]

An interesting result on systems with short-ranged attractions has been formulated by Noro and Frenkel (NF) in their so-called extended law of corresponding states.[12] According to the NF scaling law, the details of the functional form of the interaction potential are irrelevant in determining the structure and thermodynamics of fluids as long as the potential is short-ranged, i.e., the interaction range is approximately less than 15% of the particle diameter.[13] Different functional forms of the interaction yield the same behavior provided that the following three properties of the potentials are identical: σ_{eff}, ϵ, B_2^*, where σ_{eff} is the effective hard-sphere diameter of the particles which is obtained by mapping the repulsive part of the interaction $\phi(r)$ onto an effective hard-sphere (HS) diameter,[14,15] ϵ denotes the depth of the potential, i.e., $\epsilon = \phi(r_{min})$, where r_{min} is the position of the minimum, and $B_2^* = B_2/B_2^{HS}$ is the reduced second virial coefficient with $B_2^{HS} = 2\pi\sigma_{\text{eff}}^3/3$ and

$$B_2 = -2\pi \int_0^\infty (\exp(-\beta\phi(r)) - 1) r^2 dr,$$

where $\beta = 1/k_BT$ (k_B being Boltzmann's constant and T the absolute temperature). Therefore, all fluids with short-ranged interactions should yield the same thermodynamic and structural properties when compared at the same value of (ρ^*, T^*, B_2^*), where $\rho^* \equiv \rho\sigma_{\text{eff}}^3$ and $T^* \equiv k_BT/\epsilon$ are the reduced density and temperature, respectively. Although it is not a rigorous law it seems to work remarkably well. A simple corollary of NF's scaling law was observed in a preceding study by Vliegenthart and Lekkerkerker[16] who found empirically that, although the critical temperature T_c^* strongly decreases as the interaction range vanishes, the second virial coefficient $B_2^*(T_c^*)$ evaluated at the critical temperature remains practically constant, i.e., $B_2^*(T_c^*) \sim -1.5$, a relation that can be used to give a robust estimate for the critical temperature of a short-ranged system. In subsequent work, it was however found that $B_2^*(T_c^*) \sim -1.5$ is an approximation since $B_2^*(T_c^*)$ is depending on the interaction range.[1]

Various methods of statistical mechanics have been applied to study systems with short-ranged interactions: computer simulations and numerical or analytical theoretical approaches including theories based on the Ornstein Zernike (OZ) relation supplemented with a closure relation. Most of the studies have been dealing with square-well (SW)

a)Electronic mail: elisabeth.schoell-paschinger@boku.ac.at
b)Electronic mail: nextor@fisica.ugto.mx
c)Electronic mail: alb@fisica.ugto.mx
d)Electronic mail: ramoncp@fisica.ugto.mx

potentials[1,7,8]

$$\phi^{\mathrm{SW}}(r) = \begin{cases} \infty & r < \sigma \\ -\epsilon & \sigma \le r \le \lambda\sigma \\ 0 & r > \lambda\sigma \end{cases}, \tag{1}$$

where λ is the reduced range of the attraction, or hard-core attractive Yukawa potentials (HCY)[2,3,6]

$$\phi^{\mathrm{Yuk}}(r) = \begin{cases} \infty & r < \sigma \\ -\epsilon\sigma \exp(-z(r-\sigma))/r & r \ge \sigma \end{cases}, \tag{2}$$

where z is the inverse screening length.

In particular, an accurate localization of the critical temperature and the liquid-vapor coexistence curve becomes very difficult in the regime of very short-ranged interactions. However, in this regime one can refer to the so-called adhesive or sticky hard-sphere (SHS) system, a model introduced by Baxter[17] that can be interpreted as a system with vanishing interaction range and an interaction strength that is diverging in such a way that B_2^* remains finite. Baxter[17] started from the SW potential,

$$\phi^{\mathrm{BaxterSW}}(r) = \begin{cases} \infty & r < \sigma \\ -\epsilon & \sigma \le r \le \sigma(1+\delta) \\ 0 & r > \sigma(1+\delta) \end{cases}, \tag{3}$$

where $\epsilon = \beta^{-1} \ln(1 + 1/12\tau\delta)$. In the sticky limit, $\delta \to 0$, one obtains $B_2^* = 1 - 1/4\tau$, where τ is the stickiness parameter. Analytical results are available for the SHS system[17] and Monte Carlo (MC) simulations have been performed by Miller and Frenkel[20,21] that provided an estimate of the critical point parameters $\tau_c = 0.1133(5)$ and $\rho_c^* = 0.508(190)$. The approximate analytic solution within the Percus Yevick (PY) approximation,[17] however, suffers from decreasing accuracy at high densities and thermodynamic inconsistency yielding coexistence curves determined via the compressibility and the energy routes that differ significantly; the coexistence curve obtained from the energy route being in better agreement with simulation results.

One possibility to obtain the SHS limit was proposed by Baxter[17] and starts from the SW interaction of the form above (see Eq. (3)). If one starts instead with the simple HCY potential of Eq. (2), where $\epsilon = z\sigma\epsilon_0/12$ and ϵ_0 defines the energy scale, and taking the limit $z \to \infty$ keeping ϵ_0 constant, so that again the interaction range is vanishing and the strength is diverging, Gazzillo has shown for the first time in Refs. 18 and 19 and emphasized recently[22] that the exact HCY B_2^* is diverging so that the latter model is ill defined. Gazzillo also introduced an alternative model for adhesive hard-spheres called the modified HCY (mHCY) and which is obtained by taking the limit of vanishing range of the following logarithmic HCY interaction[22]

$$\phi^{\mathrm{mHCY}}(r) = \begin{cases} \infty & r < \sigma \\ -\beta^{-1} \ln\left\{1 + \frac{1}{12T^*} z\sigma^2 \exp(-z(r-\sigma))/r\right\} & r \ge \sigma \end{cases}, \tag{4}$$

where $T^* \equiv k_B T/\epsilon_0$ can be identified as the stickiness parameter τ. Asymptotically, i.e., for $r \to \infty$, the potential is identical to a HCY potential. By taking the sticky limit $z \to \infty$, $B_2^{*\mathrm{mHCY}}$ remains finite and yields $B_2^{*\mathrm{SHS}} = 1 - 1/4\tau$. Also the third virial coefficient of Baxter's SHS system is correctly reproduced.[18] It is important to emphasize that the equivalence of Baxter's SHS system and the sticky limit $z \to \infty$ of the mHCY system has been proven only up to this level and it is still an open question whether the two models fully coincide.

The thermodynamic inconsistency present in the PY solution of the SHS model, which is not able to provide quantitative predictions of the binodal curve, is no longer present when one switches to the well-known self-consistent Ornstein Zernike approximation (SCOZA),[23,24] which enforces consistency between the energy and compressibility route. SCOZA has shown to remain successful in the critical region, where usually conventional liquid-state theories fail, and has turned out to remain accurate also for short-ranged HCY and Asakura-Oosawa (AO) potentials.[3,5] Recently, SCOZA was also tested for narrow SW potentials and in the sticky limit.[8] However, in the study by Pini *et al.*[8] it was seen that the overall agreement with simulation data is not of the same accuracy as for the HCY potential. Results – especially the liquid-vapor coexistence curve – turned out to be highly sensitive to the boundary condition at high density $\rho_{\max}^* \equiv \rho_{\max}\sigma^3$, which is needed when one solves the SCOZA partial differential equation (PDE)—a fact that was already noticed in a preceding study[25] and confirmed in Ref. 8. However, this strong dependence on the high density boundary condition seems to be less dramatic when one switches to different forms of the interaction like the HCY,[3] the AO,[5] and the mHCY potential. So, in order to obtain accurate results close to the sticky limit it is more advantageous to apply SCOZA to the second model potential of Eq. (4) proposed by Gazzillo,[22] which produces – in the limit of vanishing interaction range – the second and third virial coefficients of the SHS system.[18] We have seen that for narrow mHCY systems the SCOZA solution is still depending on the high-density boundary condition, but the dependence is much less dramatic and results are no longer sensitive with respect to shifting the high density boundary condition to higher densities if we use $\rho_{\max}^* = 1.15$ for $z^* \equiv z\sigma$ values up to 18. A possible explanation for this peculiar difference of the accuracy of SCOZA for the SW and mHCY might be the fact that for the SW fluid of equivalent range the binodal curve is broader—especially the liquid branch is shifted to higher densities which could explain the larger sensitivity to the high density boundary condition as already speculated in Ref. 8.

In this article, we present SCOZA results for the mHCY system up to $z^* = 18$ which corresponds to a SW system with $\delta_{\text{eff}} = 0.056$ if we map the mHCY system at its T_c^* onto an equivalent SW system according to NF's scaling law. This interaction range is closer to the sticky limit than in the study of Pini *et al.*,[8] where the case $\delta = 0.1$ was the smallest interaction range considered. Results are compared with NVT MC simulations, i.e., simulations in the canonical ensemble where you fix the number N of particles, the volume V, and the temperature T of the system. We used the slab method to assess the accuracy of SCOZA predictions.

In Ref. 8 it was speculated that B_2^* might be diverging in the sticky limit of the SW system which seems to be a peculiarity of the SCOZA closure. Results for the mHCY system for values of z^* up to 18 do not support this speculation. Thus we treat in this article the cases $z^* \leq 18$ where this peculiarity of SCOZA – if present – is still not relevant and MC simulations are also still feasible. The investigation of z^* values closer to the sticky limit with a nonlinear SCOZA closure relation that might circumvent the divergence of B_2^* is left to future work.

The article is organized as follows. In Sec. II we introduce the logarithmic Yukawa potential. In Sec. III we present the SCOZA method for this potential. In Sec. IV details of the MC simulations are presented, and results are discussed in detail in Sec. V. Our main findings are finally summarized in Sec. VI.

II. THE LOGARITHMIC YUKAWA POTENTIAL

Gazzillo[18,22] has shown that the correct second and third virial coefficients of the adhesive hard-sphere model can be obtained by taking the limit $z \to \infty$ of the following mHCY potential:

$$\phi^{*\text{mHCY}}(r) = \frac{\phi^{\text{mHCY}}(r)}{\epsilon_0} = \begin{cases} \infty & r < \sigma \\ -T^* \ln\left\{1 + \frac{1}{12T^*} z\sigma^2 \exp(-z(r-\sigma))/r\right\} & r \geq \sigma \end{cases}, \tag{5}$$

where $T^* = \frac{k_B T}{\epsilon_0}$ corresponds to Baxter's stickiness parameter τ. The logarithmic part is the analog to the logarithmic well depth in Baxter's original SW potential of Eq. (3). The mHCY potential has the same behavior at large distances as the HCY potential where – according to the mathematical identity $\ln(1 + x) \sim x$ for $x \ll 1$ – one obtains

$$\phi^{*\text{mHCY}}(r) \sim -\frac{z\sigma^2}{12} \exp(-z(r-\sigma))/r \quad \text{for} \quad r \gg \sigma. \tag{6}$$

The difference between the HCY and the mHCY potential is largest at the contact.[22] With this definition of the potential, $B_2^*(T^*)$ no longer diverges in the sticky limit $z \to \infty$ but takes the value of Baxter's SHS system $B_2^*(T^*) = 1 - 1/4T^*$. In contrast to a pure HCY system now the potential is explicitly depending on the temperature. Thus the functional form changes with temperature which has turned out to be difficult for the numerical solution of the SCOZA PDE, where one starts at infinite temperature and integrates down to a finite temperature. During the integration with respect to β the interaction potential is changing its form. Only in the high temperature regime one recovers again a simple temperature-independent HCY potential.

III. SCOZA

SCOZA is a liquid-state theory that has proven to give accurate predictions of the liquid-vapor coexistence curves and even in the critical region, where SCOZA exhibits some form of scaling with non-classical critical exponents.[26] For a detailed description of SCOZA and its numerical solution procedure we refer the reader to the literature[23–25] and just outline here the main ideas of SCOZA. The main ingredient of SCOZA is the self-consistency requirement: most conventional microscopic liquid-state theories like integral equation theories or perturbation theories suffer from a lack of thermodynamic consistency, which means that the different statistical mechanical routes (such as the energy, the virial, and the compressibility route) from the structural properties to the thermodynamics yield more or less different results.[27,28] In SCOZA, however, self-consistency between the different routes is enforced.

The theory has been formulated in different versions for fluids interacting via a spherically symmetric pair potential $u(r)$ that consists of a hard-core of diameter σ and some attractive tail. All different versions of SCOZA grew out of the mean-spherical approximation (MSA), which like all integral equation theories is based on the Ornstein Zernike relation[27]

$$h(r) = c(r) + \rho c \otimes h(r) \tag{7}$$

that defines the direct correlation function $c(r)$ in terms of the total correlation function $h(r)$ and $\otimes$ denoting a convolution integral. A closed theory is obtained by supplementing Eq. (7) with a so-called closure relation, i.e., an approximate relation that involves $h(r)$, $c(r)$, and the interaction $u(r)$. The MSA-type closure relation of SCOZA, considered in this work, amounts to setting

$$\begin{aligned} g(r) &= 0 && \text{for} \quad r < \sigma, \\ c(r) &= A(\rho, \beta)u(r) + c_{\text{HS}}(r) && \text{for} \quad r > \sigma; \end{aligned} \tag{8}$$

where $g(r) = h(r) - 1$ is the pair distribution function, $c_{\text{HS}}(r)$ is the direct correlation function of the hard-core reference system, given, for example, by the Waisman parameterization,[29] and $A(\rho, \beta)$ is a function of the thermodynamic state (ρ, β). The first relation, the so-called core condition, is exact and corresponds to the fact that particles

are not allowed to overlap. The expression for $c(r)$ is an approximation and implies that $c(r)$ has the same range as the potential—an ansatz that is usually referred to as the OZ approximation, thus the name self-consistent Ornstein Zernike approximation. In contrast to the MSA, where $A(\rho, \beta) = -\beta$, here $A(\rho, \beta)$ is not fixed *a priori* but is instead determined to ensure thermodynamic consistency between the compressibility and the energy routes: assuming that the thermodynamics stems from a unique Helmholtz free energy the consistency condition can be expressed as

$$\frac{\partial}{\partial\beta}\left(\frac{1}{\chi^{red}}\right) = \rho\frac{\partial^2 u^{ex}}{\partial\rho^2}, \tag{9}$$

where $\chi^{red} = \rho k_B T \chi_T$ is the reduced isothermal compressibility given by the fluctuation theorem

$$\frac{1}{\chi^{red}} = 1 - \rho\tilde{c}(k=0), \tag{10}$$

where $\tilde{c}(k)$ denotes the Fourier transform of $c(r)$, and $u^{ex} \equiv \frac{U^{ex}}{V}$ is the excess (over ideal) internal energy per volume given by the energy equation

$$\frac{U^{ex}}{V} = u^{ex} = 2\pi\rho^2 \int g(r)\phi(r)r^2 dr. \tag{11}$$

The consistency equation (9) supplemented by the OZ relation (7), the closure relation (8), the compressibility route (10), and the energy route (11) yield a partial differential equation for $A(\rho, \beta)$.

When χ^{red} in Eq. (9) is expressed as a function of u^{ex} within the closure relation (8) the SCOZA PDE turns into a PDE of diffusion type for u^{ex},

$$B(\rho, u^{ex})\frac{\partial u^{ex}}{\partial\beta} = \rho\frac{\partial^2 u^{ex}}{\partial\rho^2}, \tag{12}$$

with a diffusion coefficient $B(\rho, u^{ex}) \equiv \frac{\partial}{\partial u^{ex}}(\frac{1}{\chi^{red}})$. The numerical solution procedure of SCOZA and the boundary conditions used in this work are described in detail in Ref. 25 and the finite-difference algorithm used for the numerical integration of the PDE is described in the appendix of Ref. 24.

For a long time, applications of SCOZA were limited due to historical and technical reasons; the complexity of the SCOZA formalism and the heavy numerical solution algorithm. For example, in the case of continuum fluids, applications were initially restricted to the HCY fluid where one can make use of the extensive semi-analytic MSA studies available. These semi-analytic expressions lead to simplifications of the numerical solution of SCOZA and thus a considerable reduction of computational cost. The success of SCOZA for these few model systems has motivated to broaden its applicability.[5,25,30–36] Nowadays, SCOZA is solvable for arbitrary hard-core potentials, like the AO or the SW potential.[5,25] However, in these cases the determination of the diffusion coefficient $B(\rho, u)$ must be done fully numerically and comes, of course, at a substantial computational cost.

When solving SCOZA for the modified Yukawa system with explicitly temperature-dependent potential, it turned out that the implicit finite difference algorithm became unstable when integrating the PDE with respect to the inverse temperature. So we had to turn to a different solution procedure which was coming at substantial computational cost: in order to determine the coexisting densities ρ_v^* and ρ_l^* at a given reduced temperature T^* we solved the SCOZA PDE by integrating from infinite temperature down to this temperature keeping the potential fixed at the functional form corresponding to this temperature T^*. This solution procedure was repeated for different temperature values to obtain the whole coexistence curve. We have redone the calculations for higher values of $\rho^*_{\max}$ – where the high density boundary condition is imposed – to make sure that the boundary condition was chosen at a density that is large enough that the SCOZA solution is no longer sensitive to the high density boundary condition. For the cases $z^* = 1.8, 5, 8, 10$ a boundary condition at $\rho^*_{\max} = 1$ turned out to be sufficient, for $z^* = 12, 15$ we were using $\rho^*_{\max} = 1.1$ and for the largest z^* value considered in this work, i.e., $z^* = 18$ we used $\rho^*_{\max} = 1.15$. According to NF's scaling law a value of $z^* = 18$ corresponds to an effective interaction range of $\delta_{\text{eff}} \sim 0.056$ at the critical temperature that was obtained with SCOZA. For a SW system with interaction range of $\delta = 0.1$, however, it turned out in the study of Pini *et al.*[8] that a much larger $\rho^*_{\max}$, namely $\rho^*_{\max} = 1.4$, was necessary. So compared to the SW system we are, on the one hand, able to treat shorter ranged systems with SCOZA when dealing with the mHCY system, and, on the other hand, the solution of the PDE is less sensitive to the boundary condition at high density.

Close to the critical region the numerical solution of the SCOZA PDE also turned out to be sensitive to the parameters used in the Fast Fourier Transform (FFT) technique which is required when solving numerically the OZ integral equations. This sensitivity turned out to increase when the interaction range decreased. While for the longer-ranged systems with $z^* = 1.8$ and $z^* = 5$, $N = 1024$ grid points and a grid spacing of $\Delta r^* = 0.01$ were sufficient to represent the distribution functions, we had to switch to $N = 2048$ grid points and a grid spacing of $\Delta r^* = 0.005$ for the shorter-ranged cases considered. We carefully checked whether results changed when further reducing the grid size to $\Delta r^* = 0.002$ and using $N = 8192$ grid points and found that the critical point temperature changed by less than 0.05% for the system with the shortest interaction range considered, i.e., $z^* = 18$.

IV. MONTE CARLO COMPUTER SIMULATIONS

We also study the phase coexistence by means of Monte Carlo computer simulations. In particular, we use the method developed by Chapela *et al.*[37] together with the replica exchange method.[38–40] In our simulations, we construct a parallelepiped whose dimensions are $L_y = L_x$ and $L_z = 8L_x$, where L_i with $i = x, y, z$ is the edge in the i-direction. In the center of the box, we place particles in a dense phase (phase I), surrounded by a more diluted phase (phase II). We then distribute 2727 particles in the box in such a way that the reduced total bulk density is always $\rho^* > 0.37$ and the densities in the dense and diluted phases are $\rho_I^* > 0.93$ and $\rho_{II}^* < 0.03$, respectively. In order to prepare the initial configuration we first perform a conventional MC simulation for the phase II, considering that particles interact only through the hard sphere potential. Then, we generate a homogeneous fluid

consisting on 2592 particles enclosed in a volume equal to 3/8 of the total volume of the simulation box. With this method one can prevent the crystallization of the dense phase. The remaining particles are distributed in a regular network filling the available space.

The replica exchange method is implemented as follows. We generate a set of 15 non-interacting replicas $\{S_i\}$ of the system described above, but at different temperatures T_i^* and particles interacting through the full potential described in Eq. (5). Temperatures of each replica are chosen in such a way that $T_1^* < T_2^* < \ldots < T_{15}^*$. Since the mHCY is a temperature-dependent potential, one has to take into account that the potential is different for each replica. In each system, the states are generated according to the next scheme: we randomly choose a particle which can be either displaced in the standard way or placed at a random position of the simulation box. The later operation, proposed by Lomakin *et al.*,[41] is useful to identify if the temperature of a given system is above the critical value and to avoid those T^*-values in the simulation. The acceptance ratio of standard particle displacement is fixed to 30%, while the acceptance of the second displacement could be very low. Eventually, we attempt to interchange particle configurations between replicas with a similar T^*. The acceptance probability of a configuration swap between systems is given by[42]

$$p = \min\left(1, \exp\left[(\beta_i - \beta_{i+1})\left(U\left(\mathbf{r}_i^N\right) - U\left(\mathbf{r}_{i+1}^N\right)\right)\right]\right), \quad (13)$$

where $U(\mathbf{r}_i^N)$ is the total potential energy of system S_i and $\beta_i = (k_B T_i)^{-1}$. The choice of the temperature range must ensure that the system at the highest temperature is out of the region of local minima or metastable states, i.e., the highest temperature must lie in the regime where no liquid-vapor transition is expected. Both the number of replicas and the temperature difference between replicas affect the acceptance ratio for swapping configurations.[43] In our simulations, we observe that the acceptance was around 10%.

The simulation is divided in two main stages. In the first one, the system forms either a gas or liquid phase according to its temperature (below the critical one) and its density and, in the second one, it exhibits a phase separation. Each stage consists of 10^8 MC steps, 82% are attempts to displace particles, 15% attempts to relocate particles, and the rest are attempts to swap particle configurations. During the second stage, we measure the density across the simulation box every 50 000 MC steps. In addition, we perform the simulation with ten different seeds, which improves our statistics and allows us to construct a smoother density profile $\rho(z)$. From this profile it is straightforward to calculate the densities of the coexisting phases.

To estimate the critical point, we use a scaling type law and the law of rectilinear diameters. According to this procedure the critical point parameters ρ_c and T_c are fitted to the following equations:[44]

$$\rho_l^* - \rho_v^* = C_1\left(T_c^* - T^*\right)^\beta, \quad (14)$$

$$\frac{\rho_l^* + \rho_v^*}{2} = \rho_c^* + C_2\left(T_c^* - T^*\right), \quad (15)$$

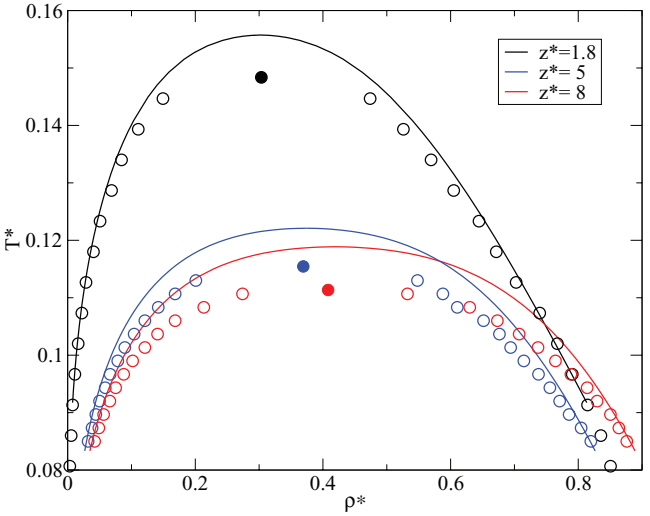

FIG. 1. Phase diagram of the mHCY fluid for reduced inverse screening length $z^* = 1.8$, $z^* = 5$, and $z^* = 8$, SCOZA (full lines), NVT computer simulations (circles): open circles for the coexistence curves and filled circles for the critical points—the error bars do not exceed the symbol size.

where ρ_l^* and ρ_v^* are the coexisting liquid and vapor densities, respectively, at given temperature T^*, $\beta = 0.325$ is the critical exponent, and C_1 and C_2 are two further fit parameters. We have used the four coexistence points that are closest to the critical point.

V. RESULTS AND DISCUSSION

A. Phase coexistence

In Figures 1 and 2, the phase diagram of the modified Yukawa potential for different values of the reduced inverse screening length z^* is shown. Furthermore, the SCOZA

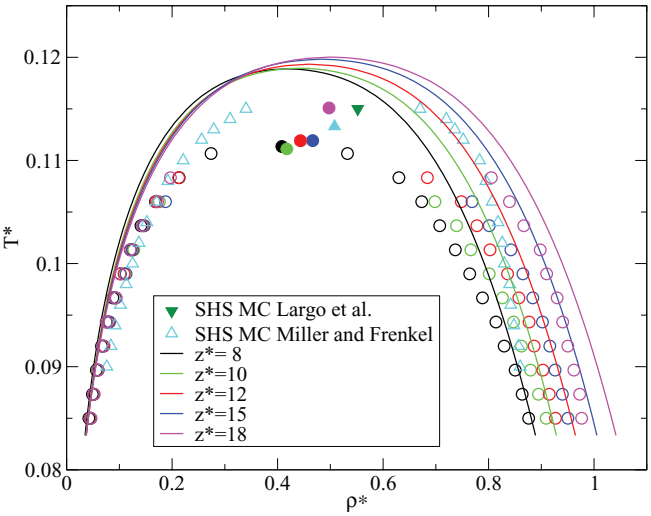

FIG. 2. Phase diagram of the mHCY fluid for reduced inverse screening length $z^* = 8$, $z^* = 10$, $z^* = 12$, $z^* = 15$, and $z^* = 18$, SCOZA (full lines), NVT computer simulations: open circles for the coexistence curves and filled circles for the critical points—the error bars do not exceed the symbol size. We also show MC simulations by Miller and Frenkel[20,21] for the SHS system (open upward triangles for the coexistence curve and full upward triangle for the critical point) and an estimate of the critical point for the SHS by Largo *et al.*[1] (full downward triangle).

TABLE I. Reduced inverse screening length z^* and reduced effective interaction range δ_{eff} of the equivalent SW system; reduced critical point parameters of SCOZA: temperature, density; reduced critical point parameters of NVT simulations: temperature, second virial coefficient, and density.

		SCOZA		MC		
z^*	δ_{eff}	T_c^*	ρ_c^*	T_c^*	B_2^{*c}	ρ_c^*
1.8	0.532	0.1557	0.302	0.1484(4)	− 1.621(6)	0.304(4)
5	0.198	0.1221	0.374	0.1155(2)	− 1.599(5)	0.369(2)
8	0.124	0.1189	0.418	0.11135(2)	− 1.5258(4)	0.408(4)
10	0.100	0.1189	0.441	0.1111(2)	− 1.475(6)	0.42(1)
12	0.083	0.1193	0.460	0.1119(3)	− 1.420(6)	0.443(3)
15	0.067	0.1198	0.480	0.1119(4)	− 1.383(9)	0.467(6)
18	0.056	0.1200	0.500	0.1151(4)	− 1.293(8)	0.498(3)

estimates for the critical parameters ρ_c^* and T_c^* are listed in Table I for the different interaction ranges considered together with NVT estimates obtained according to Eqs. (14) and (15). As we decrease the range of the interaction, i.e., with increasing z^*, the critical temperature shows a non-monotonic behavior: the critical temperature first decreases for z^* values increasing from $z^* = 1.8$ up to ∼8 and then slightly increases again. T_c^* obtained within SCOZA takes more or less a constant value of $T_c^* = 0.12$ for z^* values larger than 8. SCOZA overestimates the critical temperature, a fact that was also observed in the study by Pini *et al.*[8] for the SW system. On the other hand, for SCOZA the behavior of the critical point density is monotonic: with decreasing interaction range, i.e., increasing z^*, it also increases from $\rho_c^* = 0.302$ for $z^* = 1.8$ to $\rho_c^* = 0.500$ for $z^* = 18$, which was the largest z^* value considered in this work. In contrast to the critical temperature, which takes approximately a constant value for $z^* \geq 8$, the critical density does not take a constant value even for the smallest interaction ranges considered. So the limiting value of the SHS system is not reached yet, however, the critical density $\rho_c^* = 0.500$ is already close to $\rho_c^* = 0.508(190)$, which was predicted by MC simulations[20,21] for the SHS system. The simulation results for T_c^* show the same non-monotonic behavior. The MC estimates for ρ_c^* also increase with z^* and the limiting value of the SHS is again not reached yet. As z^* increases from 1.8 to 8 in Figure 1, the coexistence curve shifts to lower temperature and for the case $z^* = 8$ the liquid-vapor branch exhibits an unusual behavior not present in the usual Yukawa potential: the coexistence curve broadens and intersects the other coexistence curves. This behavior is due to the fact that now the mHCY is starting to show stronger deviations from the Yukawa potential and the attraction is smaller (see Figure 1 of Ref. 22). Due to the lower attraction in the mHCY system the coexisting density shifts to higher densities. MC results show the same tendency. They quantitatively agree with SCOZA predictions for the vapor and liquid branch. In Figure 2 we show the phase diagrams of the mHCY system for $z^* = 8$ up to $z^* = 18$. While the vapor branch predicted by SCOZA hardly changes, the liquid branch shifts to higher densities when increasing z^* and does not show the tendency to converge. SCOZA seems to overestimate the liquid branch. The shift of the liquid branch to higher densities is also visible in the simulations. We also show the MC predictions by Miller and Frenkel[20,21] and the critical point estimate by Largo *et al.*[1] for the SHS limit.

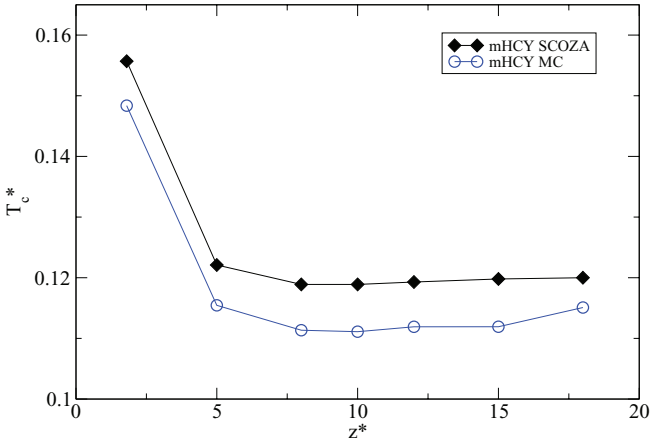

FIG. 3. The critical temperature T_c^* as a function of the inverse screening length parameter z^* for the mHCY model using SCOZA (full diamonds) and MC simulations (open circles).

In Figures 3 and 4 we show the critical parameters T_c^* and ρ_c^* as a function of the inverse screening length z^*. Both simulations and SCOZA results for T_c^* show a non-monotonic behavior. As z^* increases T_c^* first decreases and then increases again. SCOZA is, in general, overestimating the critical temperature in a systematic way. The behavior is different for the critical density, where SCOZA and MC values are increasing with z^*. Again SCOZA is overestimating the critical parameter in a systematic way. For the longest and shortest interaction range considered, i.e., $z^* = 1.8$ and $z^* = 18$, the agreement is perfect.

B. Sticky limit

In Table I, we also list the reduced second virial coefficient for the mHCY system given by

$$B_2^{*\text{mHCY}}(T^*, z^*) = 1 - \frac{1}{4T^*}\left(1 + \frac{1}{z^*}\right), \qquad (16)$$

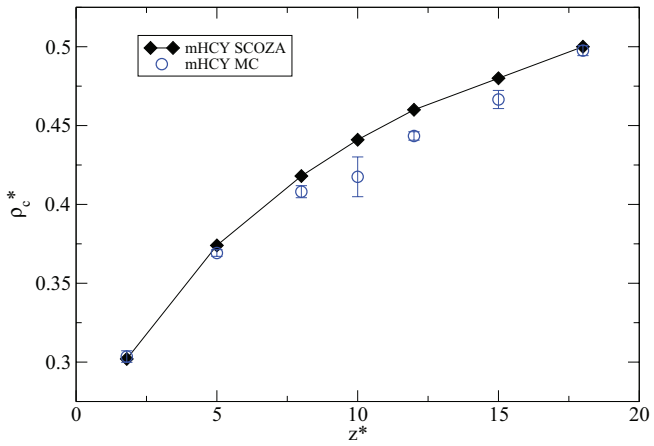

FIG. 4. The critical density ρ_c^* as a function of the inverse screening length parameter z^* for the mHCY model using SCOZA (full diamonds) and MC simulations (open circles).

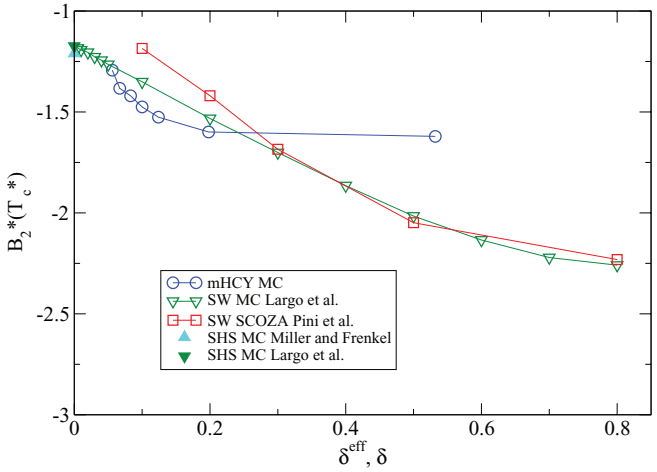

FIG. 5. Reduced second virial coefficient $B_2^*(T_c^*)$ at the critical point as a function of the effective interaction range δ_{eff} (see text) for the MC simulations of the mHCY system (circles) and as a function of the range $\delta = \lambda - 1$ of the SW system. For the latter system data are taken from Ref. 1 (open triangles) and Ref. 8 (squares). Also shown are the estimates for the SHS system from Refs. 20 and 21 (full upward triangle) and Ref. 1 (full downward triangle).

at the critical point, i.e., $B_2^{*\text{mHCY,c}} \equiv B_2^{*\text{mHCY}}(T_c^*, z^*)$. To obtain the critical second virial coefficient $B_2^{*\text{mHCY,c}}$ for the mHCY system we simply included in Eq. (16) the critical point temperature T_c^* determined with MC simulations. $B_2^{*\text{c}}$ obtained from SCOZA is only known for SW and square-shoulder systems where it is identical to the exact one,[8] otherwise it is unknown and probably different from the exact one. In order to derive an effective interaction range δ_{eff} for the mHCY system, we have applied NF's scaling law at the critical temperature of the mHCY system: it is straightforward to show that the reduced second virial coefficient of the SW potential of Eq. (1) is

$$B_2^{*\text{SW}}(T^*) = 1 - (e^{\beta\epsilon} - 1)(\lambda^3 - 1). \tag{17}$$

According to NF's scaling law, the mHCY fluid at its critical temperature T_c^* should be equivalent to a SW fluid at the same T_c^* if the second virial coefficient is identical. We furthermore have to take into account that the well depth of both potentials has to be identical. Therefore, we have to insert the potential minimum of the critical mHCY system, i.e., $\beta_c\epsilon = -\beta_c\phi^{\text{mHCY}}(\sigma, T_c^*) = \ln(1 + \frac{z^*}{12T_c^*})$ in Eq. (17) and we finally obtain the effective range of an equivalent SW fluid at the critical point temperature T_c^*:

$$\lambda_{\text{eff}}^3 = (1+\delta_{\text{eff}})^3 = 1 + \left(1 - B_2^{*\text{mHCY,c}}\right)\frac{12T_c^*}{z^*}$$
$$= 1 + \frac{3}{z^*}\left(1 + \frac{1}{z^*}\right). \tag{18}$$

This effective range δ_{eff} turns out to be fully independent of the temperature for the mHCY fluid and it is also shown in Table I.

The second virial coefficient at the critical point is plotted as a function of the effective SW range δ_{eff} for the equivalent mHCY system and as a function of δ for the SW system of Eq. (1) in Figure 5. For the latter we have used both simulation results of Largo *et al.*[1] (see Table I of this reference) and SCOZA results by Pini *et al.*[8] (see Table I therein). We used the critical temperatures in the tables and Eq. (17) to obtain $B_2^{*\text{SW,c}} = 1 - (e^{1/T_c^*} - 1)((1+\delta)^3 - 1)$.

Also shown in Figure 5 are the results for the SHS system from Refs. 20 and 21, and 1. From the figure, it becomes visible that B_2 is not constant for short-ranged potentials which is contradicting the criterion of Vliegenthart and Lekkerkerker[16] that at the critical temperature $B_2^*(T_c^*) \sim -1.5$ remains practically constant. The behavior of $B_2^*(T_c^*)$ obtained for the different systems and via all methods is in semi-quantitative agreement. In all cases, $B_2^*(T_c^*)$ increases as δ decreases. For the SW system SCOZA results by Pini *et al.*[8] and simulations by Largo *et al.*[1] are in perfect agreement for $\delta \geq 0.3$. The result obtained from the mHCY system for $\delta_{\text{eff}} = 0.532$ deviates from the other results strongly, but in this case the system cannot be considered as short-ranged and is out of the scope of NF's scaling law. As δ_{eff} decreases NF seems to work since deviations are decreasing especially around $\delta_{\text{eff}} = 0.067$. Nevertheless the simulation results for the equivalent mHCY of this work and of Largo *et al.*[1] for $\delta < 0.2$ show deviations. In the case of the simulation results for the mHCY work we cannot conclude what the fate of $B_2^*(T_c^*)$ is in the limit $\delta \to 0$ since the simulations are restricted to $\delta > 0.05$. The prediction of the liquid-vapor coexistence curve via simulations for $\delta < 0.05$ was not possible because crystallization prevented us to obtain a homogeneous liquid phase. More careful simulations for short-ranged potentials are required here.

In Figures 6 and 7 we compare the predictions of the critical density ρ_c^* and critical temperature T_c^* as a function of the effective range δ_{eff} for the mHCY system and as a function of δ for the SW system. In order to compare the critical temperatures we had to rescale the SCOZA predictions for the mHCY system according to $T_c^* \to T_c^*/\phi^{*\text{mHCY}}(\sigma) = 1/\ln(1 + z^*/12T_c^*)$. Fig. 7 shows SCOZA predictions and MC estimates for T_c^*. For $\delta \leq 0.2$ the SCOZA predictions agree well with the simulation results for the mHCY

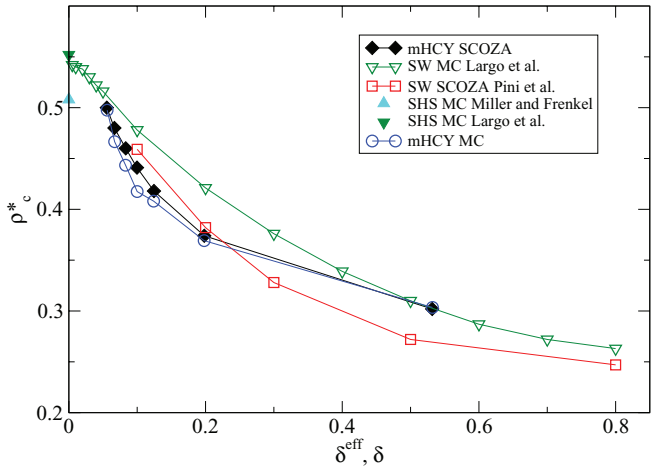

FIG. 6. Critical density ρ_c^* as a function of the effective range δ_{eff} for the mHCY model using SCOZA (diamonds) and MC simulations (circles) and as a function of δ for the SW system. For the latter system the data are taken from Ref. 1 (open triangles) and Ref. 8 (squares). We also included the corresponding values for the SHS system from Refs. 20 and 21 (full upward triangle) and Ref. 1 (full downward triangle).

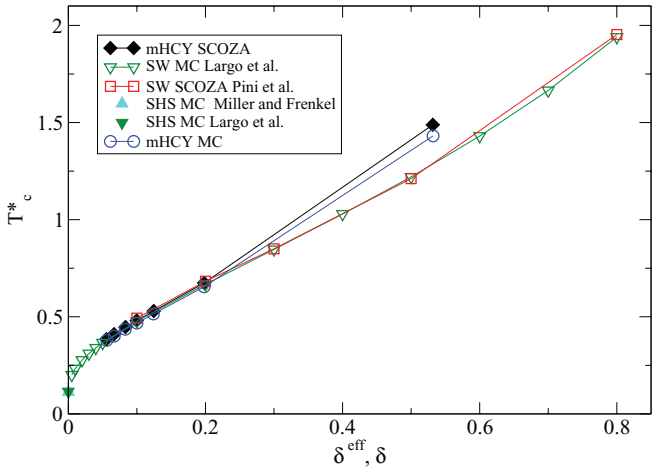

FIG. 7. The critical temperature T_c^* as a function of the effective range δ_{eff} for the mHCY model using SCOZA (diamonds) and MC simulations (circles) and as a function of δ for the SW system. For the latter system the data are taken from Ref. 1 (open triangles) and Ref. 8 (squares). We also included the corresponding values for the SHS system from Refs. 20 and 21 (full upward triangle) and Ref. 1 (full downward triangle).

system, while slight discrepancies appear for the largest δ value. For $\delta < 0.15$ the SCOZA and MC predictions for the mHCY fluid are in perfect agreement with the simulation results for the SW fluid, which confirms again that the NF scaling law is working here for short-range potentials whose attraction range is smaller than 15%.[13] In summary, we can conclude that, close to the sticky limit, SCOZA slightly overestimates the critical point temperature T_c^* and the critical density ρ_c^* when compared with MC simulations for the mHCY fluid, the discrepancy on ρ_c^* being larger than that on T_c^*. Similar observations were made for the SW system in Ref. 8. Furthermore, the tendency of SCOZA for T_c^* in the sticky limit is clearer than that for ρ_c^*.

VI. CONCLUDING REMARKS

In this work, we theoretically studied the phase behavior of the modified attractive hard-core Yukawa fluid that was introduced by Gazzillo[22] as a model potential and that does not exhibit a diverging second virial coefficient in the limit of vanishing interaction range and infinite interaction strength; it allows one to correctly reproduce B_2 and B_3 of Baxter's SHS system. We based our study on the solution of SCOZA for the modified attractive hard-core Yukawa system and concentrated on the system close to the sticky limit, i.e., for inverse screening lengths up to $z^* = 18$. Using the Noro-Frenkel extended law of scaling, we mapped this system at its critical point onto an equivalent SW fluid with an effective range and found that Noro-Frenkel's scaling law works remarkably well for interaction ranges up to 15% of the particle diameter, i.e., the SCOZA predictions for the critical temperatures and critical second virial coefficients were found to be in good agreement with simulation results for a square-well system of an effective interaction range obtained from NF's scaling law. Our results for the phase diagram and the critical parameters close to the sticky limit were explicitly compared with Monte Carlo computer simulations and good overall agreement was found.

We have demonstrated that compared to the SW model, the mHCY model allows one to obtain reliable SCOZA predictions much closer to the sticky limit. While for the first system the results are no longer reliable for $\delta < 0.1$, this is not the case for the mHCY system studied here. This might be due to the fact that the coexistence curve of the equivalent SW fluid is broader and the SCOZA solution is more sensitive to the choice of the high-density boundary condition. For the screening parameters considered here, we do not find any evidence that SCOZA yields a diverging second virial coefficient as speculated in Ref. 8 for the SW system. So a divergence of B_2 – if present – will be relevant only for very short-ranged potentials closer to the sticky limit.

ACKNOWLEDGMENTS

This work was supported by the Elise Richter project V132-N19 of the Austrian Science Fund (FWF). Part of the calculations were carried out on the Vienna Scientific Cluster (VSC). A.L.B. and R.C.P. are grateful for financial support from PIFI 2012, PROMEP (Red Física de la Materia Blanda), and CONACyT (Grant No. 102339/2008). The authors appreciate helpful explanations of D. Gazzillo about his potential.

[1] J. Largo, M. A. Miller, and F. Sciortino, J. Chem. Phys. **128**, 134513 (2008).
[2] G. Foffi, G. D. McCullagh, A. Lawlor, E. Zaccarelli, K. A. Dawson, F. Sciortino, P. Tartaglia, D. Pini, and G. Stell, Phys. Rev. E **65**, 031407 (2002).
[3] P. Orea, C. Tapia-Medina, D. Pini, and A. Reiner, J. Chem. Phys. **132**, 114108 (2010).
[4] S. Buzzaccaro, R. Rusconi, and R. Piazza, Phys. Rev. Lett. **99**, 098301 (2007).
[5] N. E. Valadez-Pérez, A. L. Benavides, E. Schöll-Paschinger, and R. Castaneda-Priego, J. Chem. Phys. **137**, 084905 (2012).
[6] A. Malijevsky, S. B. Yuste, and A. Santos, J. Chem. Phys. **125**, 074507 (2006).
[7] M. Dijkstra, Phys. Rev. E **66**, 021402 (2002).
[8] D. Pini, A. Parola, J. Colombo, and L. Reatto, Mol. Phys. **109**, 1343 (2011).
[9] C. Gogelein, D. Wagner, F. Cardinaux, G. Nägele, and S. U. Egelhaaf, J. Chem. Phys. **136**, 015102 (2012).
[10] A. P. R. Eberle, N. J. Wagner, and R. Castaneda-Priego, Phys. Rev. Lett. **106**, 105704 (2011).
[11] J. M. Kim, J. Fang, A. P. R. Eberle, R. Castaneda-Priego, and N. J. Wagner, Phys. Rev. Lett. **110**, 208302 (2013).
[12] M. G. Noro and D. Frenkel, J. Chem. Phys. **113**, 2941 (2000).
[13] D. Frenkel, Science **314**, 768 (2006).
[14] H. C. Andersen, J. D. Weeks, and D. Chandler, Phys. Rev. A **4**, 1597 (1971).
[15] J. A. Barker and D. Henderson, Rev. Mod. Phys. **48**, 587 (1976).
[16] G. A. Vliegenthart and H. N. W. Lekkerkerker, J. Chem. Phys. **112**, 5364 (2000).
[17] R. J. Baxter, J. Chem. Phys. **49**, 2770 (1968).
[18] D. Gazzillo and A. Giacometti, Mol. Phys. **101**, 2171 (2003).
[19] D. Gazzillo and A. Giacometti, J. Appl. Crystallogr. **36**, 832 (2003).
[20] M. A. Miller and D. Frenkel, Phys. Rev. Lett. **90**, 135702 (2003).
[21] M. A. Miller and D. Frenkel, J. Chem. Phys. **121**, 535 (2004).
[22] D. Gazzillo, J. Chem. Phys. **134**, 124504 (2011).
[23] D. Pini, G. Stell, and N. B. Wilding, Mol. Phys. **95**, 483 (1998).
[24] D. Pini, G. Stell, and R. Dickman, Phys. Rev. E **57**, 2862 (1998).
[25] E. Schöll-Paschinger, A. L. Benavides, and R. Castañeda-Priego, J. Chem. Phys. **123**, 234513 (2005).
[26] J. S. Høye, D. Pini, and G. Stell, Physica A **279**, 213 (2000).
[27] J. P. Hansen and I. R. McDonald, *Theory of Simple Liquids*, 2nd ed. (Academic Press, New York, 1986).
[28] C. Caccamo, Phys. Rep. **274**, 1 (1996).
[29] E. Waisman, Mol. Phys. **25**, 45 (1973).

[30]G. Kahl, E. Schöll-Paschinger, and G. Stell, J. Phys.: Condens. Matter **14**, 9153 (2002).
[31]E. Schöll-Paschinger, J. Chem. Phys. **120**, 11698 (2004).
[32]D. Costa, G. Pellicane, C. Caccamo, E. Schöll-Paschinger, and G. Kahl, Phys. Rev. E **68**, 021104 (2003).
[33]E. Schöll-Paschinger and G. Kahl, J. Chem. Phys. **123**, 134508 (2005).
[34]E. Schöll-Paschinger, D. Levesque, J.-J. Weis, and G. Kahl, J. Chem. Phys. **122**, 024507 (2005).
[35]E. Schöll-Paschinger and A. Reiner, J. Chem. Phys. **125**, 164503 (2006).
[36]F. F. Betancourt-Cardenas, L. A. Galicia-Luna, A. L. Benavides, J. A. Ramirez, and E. Schöll-Paschinger, Mol. Phys. **106**, 113 (2008).
[37]G. A. Chapela, S. E. Martínez-Casas, and C. Varea, J. Chem. Phys. **86**, 5683 (1987).
[38]R. H. Swendsen and J. S. Wang, Phys. Rev. Lett. **57**, 2607 (1986).
[39]C. J. Geyer, in *Computing Science and Statistics: Proceedings of the 23rd Symposium on the Interface* (American Statistical Association, New York, 1991), p. 156.
[40]K. Hukushima and K. Nemoto, J. Phys. Soc. Jpn. **65**, 1604–1608 (1996).
[41]A. Lomakin, N. Asherie, and G. B. Benedek, J. Chem. Phys. **104**, 1646 (1996).
[42]D. J. Earl and M. W. Deem, Phys. Chem. Chem. Phys. **7**, 3910–3916 (2005).
[43]N. Rathore, M. Chopra, and J. J. de Pablo, J. Chem. Phys. **122**, 024111 (2005).
[44]A. Z. Panagiotopoulos, *Observation, Prediction and Simulation of Phase Transitions in Complex Fluids*, NATO ASI Series C Vol. 460 (Kluwer Academic Publishers, Dordrecht, The Netherlands, 1995), pp. 463–501.